JGR Biogeosciences

RESEARCH ARTICLE
10.1029/2021JG006264

Key Points:

- Built a biogeochemical reaction model to predict the rate response of anaerobic organic matter decomposition to temperature variations
- Decomposition rate increases almost linearly with temperature from 5°C to 30°C, which contradicts the exponential relationship of Q_{10} approach
- Q_{10} coefficient of anaerobic organic matter decomposition decreases from >400 at around 0°C to near 1 at 30°C

Supporting Information:

Supporting Information may be found in the online version of this article.

Correspondence to:

Q. Jin,
qjin@uoregon.edu

Citation:

Wu, Q., Ye, R., Bridgham, S. D., & Jin, Q. (2021). Limitations of the Q_{10} coefficient for quantifying temperature sensitivity of anaerobic organic matter decomposition: A modeling based assessment. *Journal of Geophysical Research: Biogeosciences*, *126*, e2021JG006264. https://doi.org/10.1029/2021JG006264

Received 29 JAN 2021
Accepted 26 JUL 2021

Limitations of the Q_{10} Coefficient for Quantifying Temperature Sensitivity of Anaerobic Organic Matter Decomposition: A Modeling Based Assessment

Qiong Wu[1], Rongzhong Ye[2,3], Scott D. Bridgham[3], and Qusheng Jin[1]

[1]Department of Earth Science, University of Oregon, Eugene, OR, USA, [2]Department of Plant and Environmental Sciences, Pee Dee Research and Education Center, Clemson University, Florence, SC, USA, [3]Institute of Ecology and Evolution, University of Oregon, Eugene, OR, USA

Abstract The Q_{10} coefficient is the ratio of reaction rates at two temperatures 10°C apart, and has been widely applied to quantify the temperature sensitivity of organic matter decomposition. However, biogeochemists and ecologists have long recognized that a constant Q_{10} coefficient does not describe the temperature sensitivity of organic matter decomposition accurately. To examine the consequences of the constant Q_{10} assumption, we built a biogeochemical reaction model to simulate anaerobic organic matter decomposition in peatlands in the Upper Peninsula of Michigan, USA, and compared the simulation results to the predictions with Q_{10} coefficients. By accounting for the reactions of extracellular enzymes, mesophilic fermenting and methanogenic microbes, and their temperature responses, the biogeochemical reaction model reproduces the observations of previous laboratory incubation experiments, including the temporal variations in the concentrations of dissolved organic carbon, acetate, dihydrogen, carbon dioxide, and methane, and confirms that fermentation limits the progress of anaerobic organic matter decomposition. The modeling results illustrate the oversimplification inherent in the constant Q_{10} assumption and how the assumption undermines the kinetic prediction of anaerobic organic matter decomposition. In particular, the model predicts that between 5°C and 30°C, the decomposition rate increases almost linearly with increasing temperature, which stands in sharp contrast to the exponential relationship given by the Q_{10} coefficient. As a result, the constant Q_{10} approach tends to underestimate the rates of organic matter decomposition within the temperature ranges where Q_{10} values are determined, and overestimate the rates outside the temperature ranges. The results also show how biogeochemical reaction modeling, combined with laboratory experiments, can help uncover the temperature sensitivity of organic matter decomposition arising from underlying catalytic mechanisms.

Plain Language Summary The Q_{10} coefficient is a key parameter for quantifying the temperature sensitivity of organic matter decomposition. Most modeling studies fix the Q_{10} coefficient at a constant of 1.5 or 2, assuming that decomposition rates increase by a factor of 1.5 or 2 per 10°C increase, respectively. However, the Q_{10} coefficients obtained from laboratory and field experiments are not constant, varying from less than 2 to over 300. We evaluated the constant Q_{10} approach by simulating anaerobic organic matter decomposition in peatlands in the Upper Peninsula of Michigan, USA. Our biogeochemical reaction model was constructed and validated on the basis of previous laboratory incubation experiments, and accounts for the reactions of extracellular enzymes, mesophilic fermenting and methanogenic microbes, and their temperature responses. The modeling results show that organic matter decomposition responds almost linearly to temperature variations between 5°C and 30°C, and the resulting Q_{10} coefficients decrease from >400 around 0°C to close to 1 at 30°C. These results challenge Q_{10} coefficient as an effective parameter for studying organic matter decomposition, and suggest that biogeochemical reaction modeling, combined with laboratory experiments, can be applied to discover the temperature responses of decomposition arising from underlying enzymatic and microbial reaction mechanisms.

1. Introduction

Soil organic matter is one of the largest carbon reservoirs, and its decomposition plays a key role in biogeochemical carbon cycling. At a global scale, organic matter decomposition drives annual fluxes of 210 Gt

carbon dioxide (CO_2) and 0.6 Gt methane (CH_4) into the atmosphere, directly contributing to the CO_2 and CH_4 accumulation in the atmosphere and the resulting global warming by the greenhouse effect (Ciais et al., 2013; Jackson et al., 2020; Thauer et al., 2008). In return, surface warming speeds up the reactions of enzymes and microbes participating in organic matter decomposition, leading to a positive feedback (Gill et al., 2017; Hopple et al., 2020; Romero-Olivares et al., 2017). Therefore, models that predict how organic matter decomposition responds to temperature changes play an integral role in simulating the dynamics of soil carbon storage and the fluxes of carbon cycles, and for forecasting future climate (Allison et al., 2010; Todd-brown et al., 2018; Zheng et al., 2019).

To describe the temperature sensitivity of organic matter decomposition, most models have used versions of the van't Hoff's temperature coefficient Q_{10},

$$Q_{10} = \left(\frac{r_1}{r_o}\right)^{\frac{10}{\Delta T}}. \quad (1)$$

Here r_o and r_1 are the rates of organic matter decomposition at temperature T_o and T_1, respectively, and ΔT is the difference between the two temperatures (van't Hoff, 1898). The Q_{10} coefficient can be intrinsic where the temperature sensitivity arises primarily from the inherent kinetic properties of organic compounds, or apparent if the temperature response is also shaped by the physicochemical heterogeneity and biological processes, such as in laboratory and field experiments (Davidson & Janssens, 2006; Perkins et al., 2012). Most applications fix the Q_{10} coefficient at a constant of 1.5 or 2, assuming that decomposition rates increase by a factor of 1.5 or 2 per 10°C increase, respectively (Foereid et al., 2014; von Lützow & Kögel-Knabner, 2009). However, the constant Q_{10} approach has proven repeatedly to be inconsistent with laboratory and field observations. For example, the apparent Q_{10} coefficients obtained from laboratory and field studies are not constant, but decrease from >300 at ~0°C to near 2 around 25°C (Hamdi et al., 2013).

The Q_{10} approach assumes that reaction rates increase exponentially with temperatures. This assumption originates from the transition state theory for elementary reactions (Eyring, 1935), but its application to complex processes, such as organic matter decomposition, is problematic. Specifically, organic matter decomposition consists of a series of reactions catalyzed by extracellular enzymes and fermenting and respiring microbes, and its rates are often assumed to be limited by the fermentative degradation of complex organic molecules (Allison et al., 2010; Roy Chowdhury et al., 2015; Zheng et al., 2019). Like other microbially catalyzed reactions, fermentative reactions respond to temperature variations by following unimodal functions (Finke & Jørgensen, 2008; Parashar et al., 1993). Therefore, rates of organic matter decomposition may not vary exponentially with temperatures (Fissore et al., 2008; Hagerty et al., 2014; Hopkins et al., 2014; Raich et al., 2006). Nevertheless, model practitioners continue to use constant Q_{10} coefficients routinely, perhaps because the uncertainty inherent in forecasting the progress of organic matter decomposition outweighs the error introduced by the Q_{10} approach.

The temperature response of organic matter decomposition can also be investigated by biogeochemical reaction modeling. This approach breaks organic matter decomposition into a reaction network that consists of enzymatic and microbial reactions, and simulates numerically the decomposition progress according to the rate laws of enzymatic and microbial reactions (Jin & Roden, 2011). Typical network reactions include the conversion of soil organic matter (SOM) to dissolved organic carbon (DOC) by extracellular enzymes, fermentation reactions that consume DOC, and respiration reactions that oxidize fermentation products by reducing dioxygen (O_2), sulfate, and other electron acceptors (Allison et al., 2010; Schink, 1997; Zheng et al., 2019). This modeling approach does not assume a priori how organic matter decomposition responds to variations in temperature. Instead, it uses rate laws to relate individual enzymatic and microbial rates to temperature, pH, nutrient concentrations, and other environmental conditions. By integrating the rate laws forward over time, the modeling approach simulates the temperature sensitivity of organic matter decomposition as a systems property that emerges from the interactions between enzymatic and microbial reactions under the constraints of the quality and availability of organic matter and other environmental conditions.

Here, we examine the temperature sensitivity of anaerobic organic matter decomposition by comparing the results of the Q_{10} approach with those of biogeochemical reaction modeling. We use as an example

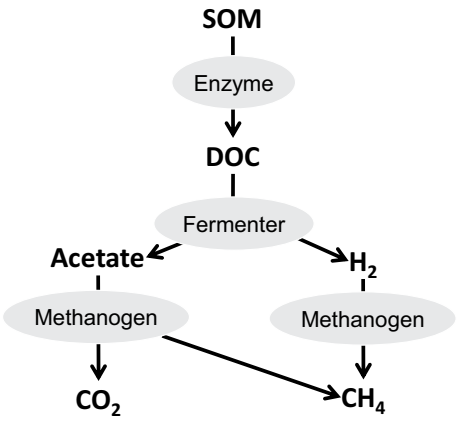

Figure 1. Anaerobic organic matter decomposition to CO_2 and CH_4. soil organic matter (SOM), and dissolved organic carbon (DOC) are soil organic matter and dissolved organic carbon, respectively; ovals indicate extracellular enzyme and microbial functional groups.

anaerobic organic matter decomposition in peatlands in the Upper Peninsula of Michigan, USA (Ye et al., 2016). Unlike previous efforts, we focus not on Q_{10} estimation or the influences of physicochemical or biological conditions of the environment, but on how the choice of an approach for describing the temperature sensitivity might affect the rate predictions of organic matter decomposition, and hence the fluxes of carbon cycling.

2. Methods

2.1. Q_{10} Approach

The Q_{10} approach treats organic matter decomposition as a black box, and provides a simple means of quantifying temperature sensitivity of decomposition rate. At temperature T, decomposition rate r can be related to the base rate r_o at base temperature T_o according to

$$r = r_o \cdot Q_{10}^{\left(\frac{T-T_o}{10}\right)}. \tag{2}$$

Therefore, the application of the Q_{10} approach requires the base rate r_o and the Q_{10} coefficient determined at base temperature T_o.

2.2. Biogeochemical Reaction Model

Anaerobic microbial decomposition of organic matter consists of a series of reactions catalyzed by extracellular enzymes and microbes. In the simplest possible configuration (Figure 1), four reactions would be required to decompose organic matter to CO_2 and CH_4. The first is the degradation of SOM to DOC by extracellular enzymes, followed by the fermentation reaction that consumes DOC and produces acetate and dihydrogen (H_2), and by the methanogenesis reactions that consume acetate and H_2 (Schink, 1997; Zheng et al., 2019). This model is applicable to an environment where O_2, ferric minerals, oxidized humic substances, sulfate, and other electron acceptors are absent and the reduction of these electron acceptors contribute little to the consumption of acetate and H_2.

Rates of SOM degradation to DOC depend on the concentrations of SOM and extracellular enzymes and can be described according to the Michaelis-Menten equation. We assume that extracellular enzymes are produced primarily by fermenting microbes and that their production and decay are at steady state (Aderibigbe & Odunfa, 1990; Burns et al., 2013; Gueguen et al., 1995). We also assume that SOM degradation is inhibited by the accumulation of DOC. Based on these assumptions, we relate enzyme concentrations to the biomass concentrations $[X_F]$ of fermenting microbes (see Text S1), and calculate the rates of SOM degradation r according to the revised Michaelis-Menten equation,

$$r = k \cdot \left[X_F\right] \cdot \frac{m_{SOM}}{m_{SOM} + K_{m,SOM}} \cdot \max\left(1 - \frac{m_{DOC}}{m_{DOC,o}}, 0\right). \tag{3}$$

Here, k is the rate constant (mol · g-biomass^{-1} · s^{-1}), m_{SOM} and m_{DOC} are the molal concentrations of SOM and DOC, respectively, $K_{m,SOM}$ is the Michaelis constant, and $m_{DOC,o}$ is the threshold DOC concentration above which the synthesis of the extracellular enzymes stops. This equation simplifies to

$$r = k_{app} \cdot \left[X_F\right] \cdot \max\left(1 - \frac{m_{DOC}}{m_{DOC,o}}, 0\right), \tag{4}$$

where $m_{SOM} >> K_{m,SOM}$, or SOM concentrations remain nearly constant. Here k_{app} is the apparent rate constant. Under these conditions, the effect of SOM concentrations can be safely neglected.

We represent microbial reactions using stoichiometric equations, and calculate their rates by using the modified Monod equation (Jin & Bethke, 2003, 2005). Specifically, the fermentation reaction is,

$$DOC \rightarrow a\text{Acetate} + bH_2 + cCO_2 + dH_2O + eH^+, \tag{5}$$

where DOC is represented using a generic chemical formula of $C_6H_{12}O_6$, and a and others are stoichiometric coefficients (Tang et al., 2016). Acetoclastic methanogenesis is

$$\text{Acetate} + H_2O \rightarrow CO_2 + CH_4. \tag{6}$$

Hydrogenotrophic methanogenesis is

$$4H_2 + CO_2 \rightarrow 2H_2O + CH_4. \tag{7}$$

Rates r of microbial reactions are calculated according to

$$r = k \cdot f_T \cdot [X] \cdot F_K \cdot F_T, \tag{8}$$

where k is the rate constant, or cell-specific maximum rate (mol · g-biomass^{-1} · s^{-1}), f_T is the dimensionless factor that describes the temperature response of the rate, [X] is the biomass concentration, F_K is the kinetic factor, and F_T is the thermodynamic potential factor. The kinetic factor accounts for nutrient concentration m_N (molal),

$$F_K = \frac{m_N}{m_N + K_N}, \tag{9}$$

where K_N is the half-saturation constant. The thermodynamic factor considers the Gibbs free energy change ΔG (J · mol^{-1}) of microbial reactions,

$$F_T = 1 - \exp\left(\frac{\Delta G + \nu_P \cdot \Delta G_P}{\chi RT}\right). \tag{10}$$

Here ν_P is the ATP yield, the number of ATPs synthesized per microbial reaction, ΔG_P is the phosphorylation energy (the energy consumed by ATP synthesis in the cytoplasm with a value of 45 kJ · mol^{-1}), χ is the average stoichiometric number, R is the gas constant (8.3145 J · mol^{-1} · K^{-1}), and T is the absolute temperature. The Gibbs free energy change is calculated from the reaction quotient Q and equilibrium constant K according to

$$\Delta G = RT \ln\frac{Q}{K}. \tag{11}$$

Variations in the equilibrium constants with temperature are shown in Figure S1.

Evaluating Equation 8 requires biomass concentrations [X], which are calculated by using the modified logistic equation. Taking the biomass concentration [X_F] of fermenting microbes as an example,

$$\frac{d[X_F]}{dt} = Y \cdot r \cdot \left(1 - \frac{[X_F]}{[X_F]_{max}}\right) - D \cdot [X_F], \tag{12}$$

where Y is the biomass yield (g · mol^{-1}), the amount of biomass synthesized per reaction, $[X_F]_{max}$ is the maximum biomass concentration supported by the environment, and D is the maintenance rate (s^{-1}). Here the maintenance rate accounts for the decrease in growth rate due to cellular maintenance, that is, metabolic processes that maintain the integrity and function of cellular components but do not contribute to the production of new cells (Hoehler & Jørgensen, 2013).

2.3. Temperature Responses

Unimodal temperature responses are key features of enzymatic and microbial reactions. In general, enzymatic and microbial reaction rates first increase with increasing temperature and, after reaching maximum values at their optimal temperatures, the rates start to decrease. Such temperature responses have been described by both mechanistic and phenomenological models (Alster et al., 2016; DeLong et al., 2017; Rossol et al., 1993; Schipper et al., 2014).

We describe the temperature responses of extracellular enzymes according to the enzyme-assisted Arrhenius equation (DeLong et al., 2017). This equation differs from the standard Arrhenius equation by

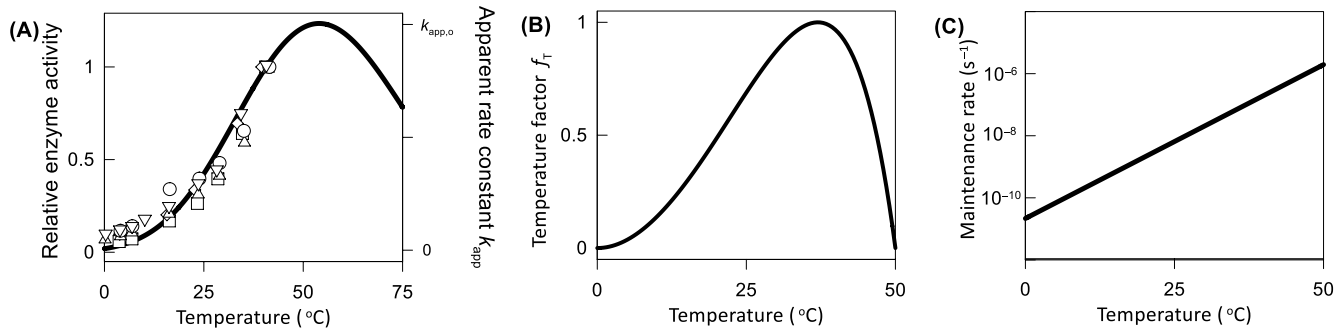

Figure 2. Variations with temperature in the relative activities and the apparent rate constant k_{app} of extracellular enzymes from soils reported by previous laboratory studies (A), the temperature factor f_T of microbial reactions (B), and maintenance rate (C). In panel A, data points are relative activities of N-acetyl-glucosaminidase (▽), cellobiohydrolase (□), β-xylosidase (◇), β-glucosidase (△), and α-glucosidase (□), calculated as the ratios of enzyme reaction rates to those determined at 40°C (Stone et al., 2012), line is the best-fit of Equation 13, and $k_{app,o}$ stands for the maximum rate constant at 57°C. In panel (B), factor f_T is calculated according to Equation 14 and by taking the minimum, optimal, and maximum temperature at 0, 37 and 50°C, respectively.

accounting for the temperature-dependent protein unfolding or denaturation. It gives the apparent rate constant of extracellular enzymes as

$$k_{app} = k_{app,o} \cdot \exp\left\{-\frac{1}{RT}\left[E_b - E_{\Delta H}\left(1-\frac{T}{T_m}\right) - E_{\Delta Cp}\left(T - T_m - T\ln\frac{T}{T_m}\right)\right]\right\}. \quad (13)$$

Here $k_{app,o}$ is the maximum apparent rate constant, E_b, $E_{\Delta H}$, and $E_{\Delta Cp}$ are the baseline activation energy (J · mol^{-1}), the change in the activation energy due to the enthalpy of enzyme folding, and the change from the change in heat capacity of the enzymes, respectively, and T_m is the melting temperature of the enzymes (K). The values of E_b, $E_{\Delta H}$, and $E_{\Delta Cp}$ delineate the temperature responses of enzyme reactions (Figure 2A), and are estimated based on laboratory observations of the enzymes harvested from mesophiles. Based on Feller (2010), we take T_m, $E_{\Delta H}$, and $E_{\Delta Cp}$ as 66°C, 59 kJ · mol^{-1} and 2 kJ · mol^{-1} · K^{-1}, respectively. We estimate the E_b value by fitting Equation 13 to temperature response of extracellular enzymes reported by Stone et al. (2012). The best-fit E_b is 36.5 ± 1.94 kJ · mol^{-1} (mean ± 95% confidence interval). As shown in Figure 2A, the equation captures the temperature responses of the different extracellular enzymes.

We describe the temperature responses of fermentation and methanogenesis by using the cardinal temperature model, a phenomenological equation (Rossol et al., 1993). According to this model, the temperature factor f_T of microbial reactions can be calculated as

$$f_T = \max\left\{0, \frac{(T-T_{max})(T-T_{min})^2}{(T_{opt}-T_{min})\left[(T_{opt}-T_{min})(T-T_{opt}) - (T_{opt}-T_{max})(T_{opt}+T_{min}-2T)\right]}\right\}. \quad (14)$$

Here, T_{min}, T_{opt}, and T_{max} are the minimum, optimal, and maximum temperature, respectively. Compared to other phenomenological models (Heitzer et al., 1991; Ratkowsky et al., 1983; Rossol et al., 1993), the cardinal temperature model is unique in that it describes microbial temperature responses by taking cardinal temperatures as input, without the need of additional parameters. Figure 2B shows, according to the cardinal temperature model, how the temperature factor f_T varies with temperature.

Other unimodal models, such as the enzyme-assisted Arrhenius model (DeLong et al., 2017) and the macromolecular rate theory (Schipper et al., 2014), can also be used to describe the temperature response of microbial reactions. These models build on kinetic theories of enzyme catalysis, and their applications require parameters related to the thermokinetic properties of enzymes and their reactions, which are not available for most microbial reactions. Therefore, their applications are currently limited. Furthermore, microbial reactions are catalyzed by tens to hundreds of enzymes and, according to metabolic control theory, their rates are not controlled by a single rate-limiting enzyme, but by multiple enzymes at the same time (Fell, 1992). Considering that different enzymes tend to display different thermokinetic properties and activity levels, and that interactions among enzymes are nonlinear, direct application of enzyme kinetic theories to complex microbial reactions can be problematic. On the other hand, the cardinal temperature model does not

Table 1
Kinetic and Thermodynamic Parameters of Microbial Reactions

	Kinetic parameter					Thermodynamic parameter	
Reaction (substrate)	Initial biomass ($mg \cdot kg^{-1}$)	Rate constant k ($mol \cdot g^{-1} \cdot s^{-1}$)	Half-saturation constant K_N (molal)	Growth yield Y ($g \cdot mol^{-1}$)	Maximum biomass ($mg \cdot kg^{-1}$)	Average stoichiometric number χ	ATP yield
Fermentation (DOC; glucose)	0.20 ± 0.13[a]	5×10^{-6} (DOC); 2×10^{-5} (glucose)[b]	1×10^{-3}[c]	10.0	0.5 ± 0.01[a]	1[d]	2[e]
Methanogenesis (acetate)	1.85 ± 0.17[a]	2.9×10^{-6}[f]	1×10^{-5}[g]	1.0	20[h]	2[f]	0.2[f]
Methanogenesis (H_2)	7.0 ± 0.13[a]	7.4×10^{-6}[f]	1×10^{-7}[g]	1.25	20[h]	2[f]	0.25[f]

[a]Determined by this study (mean ±95% confidence interval). [b]Shiloach et al. (1996). [c]Kim et al. (2007). [d]Assuming that glucose uptake is the rate-determining step. [e]Lee et al. (2008). [f]Jin and Kirk (2018). [g]Hungate (1967); Stams et al. (2003). [h]Jiang et al. (2010).

consider underlying catalytic mechanisms of microbial reactions, but reproduces well the temperature responses of microbial reactions, which is adequate for our purpose, to predict the temperature sensitivity of organic matter decomposition from the temperature responses of individual reaction steps.

No mechanistic or phenomenological model is available to calculate the maintenance rate at different temperatures. According to the microbial maintenance rates at different temperatures compiled by Price and Sowers (2004), maintenance rates D vary exponentially with temperature, which can be described with the Arrhenius equation (Figure 2C),

$$D = A_D \cdot \exp\left(\frac{-E_{a,D}}{RT}\right). \quad (15)$$

Here, A_D is the preexponential factor (s^{-1}), and $E_{a,D}$ is the apparent activation energy ($J \cdot mol^{-1}$). Based on the data compiled by Price and Sowers (2004), we set A_D at 2.5×10^{10} s^{-1} and E_D at 1.02×10^2 $kJ \cdot mol^{-1}$.

2.4. Sensitivity Analysis

Following the framework of metabolic control analysis (Fell, 1992), we conducted a sensitivity analysis to analyze the significance by which the kinetic parameters of extracellular enzymes and microbes control the rates of anaerobic organic matter decomposition. The scaled control coefficient ε_p^r of a parameter p on the rate r is the ratio of the fractional change in the rate to the fractional increase of the parameter,

$$\varepsilon_p^r = \frac{p}{r} \cdot \frac{\partial r}{\partial p}. \quad (16)$$

A coefficient of 0 indicates that the rate of anaerobic organic matter decomposition is insensitive to the parameter. A value of unity occurs where the rate varies proportionally to the changes of the parameter, indicating a strong control.

2.5. Model Application

We implemented the biogeochemical reaction model with PHREEQC (version 3.0), a software package for geochemical and biogeochemical reaction modeling (Charlton & Parkhurst, 2011). We amended its thermodynamic database by adding SOM and DOC. The amended thermodynamic database and the input scripts are available at https://zenodo.org/record/4480176 (Wu et al., 2021a). Table 1 lists the parameters and their values for computing microbial reaction rates. Some parameter values are taken directly from previous laboratory studies, whereas other parameters, including the maximum apparent rate constant $k_{ap,o}$ of extracellular enzymes, the minimum and optimal temperature of the cardinal model, and the initial biomass concentrations of fermenting and methanogenic microbes, depend on the field site of interest and are determined based on previous experimental observations. Note that due to the limited experimental

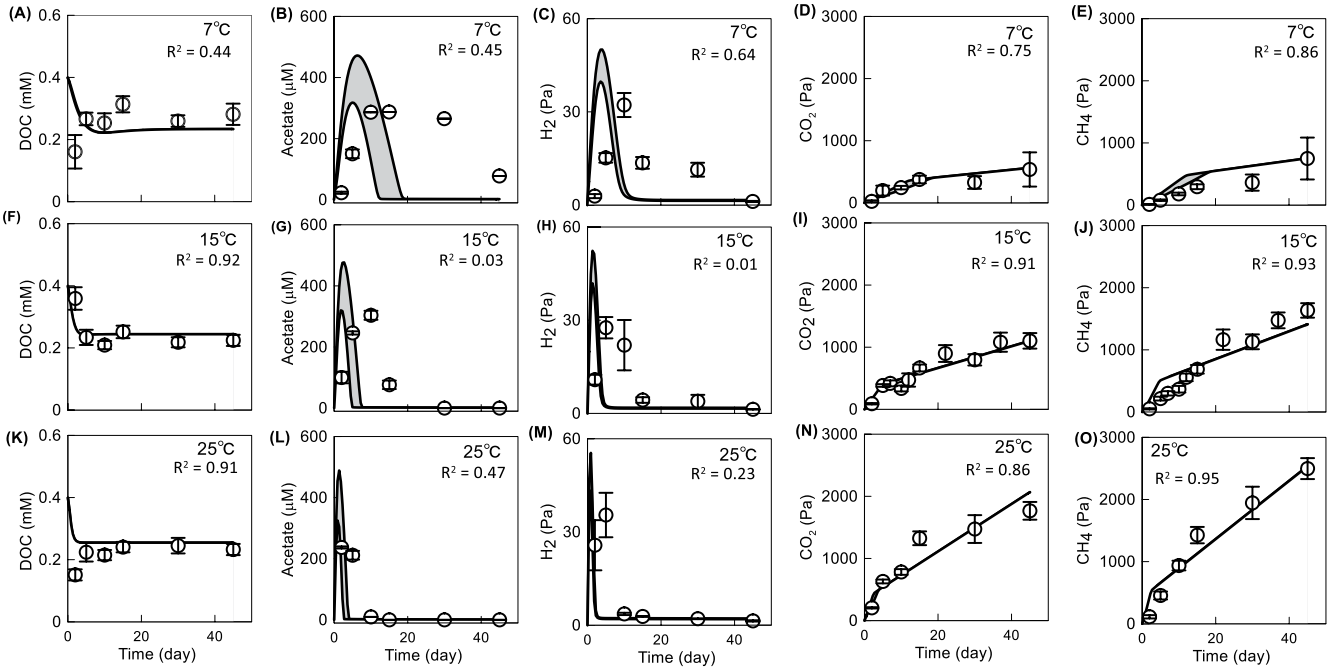

Figure 3. Parameter estimation by fitting the modeling results to the variations with time in the concentrations of dissolved organic carbon (DOC), as represented by glucose empirically (A, F, K), acetate (B, G, L), H_2 (C, H, M), CO_2 (D, I, N), and CH_4 (E, J, O) in the experiments of organic matter decomposition with glucose amendment at 7°, 15° and 25°C. Data points are the experimental observations of Ye et al. (2016); error bars show the 95% confidence intervals of the observations; solid lines and shaded areas are the simulation results by using the minimum and maximum initial biomass concentrations (see Table 1).

observations at temperatures above 25°C, we fix T_{max} of the cardinal model at 50°C (Kolton et al., 2019; Singh & Das, 2019).

We built the biogeochemical reaction model on the basis of the laboratory experiments conducted by Ye et al. (2016). Ye et al. (2016) sampled peatlands from the Upper Peninsula of Michigan, USA (sampling site, rich fen), and incubated the peat slurries anaerobically for 45 days. They included six independent sets of experiments, with and without glucose amendment at 7°C, 15°C, and 25°C in quadruplicate. They monitored the concentrations of both intermediate and final products of anaerobic organic matter decomposition, including DOC, acetate, H_2, CO_2, and CH_4 (Figures 3 and 4). According to their results, the SOM decomposition can be represented by a simple reaction network, including enzymatic reaction that hydrolyzes SOM to DOC, the fermentation reaction that consumes DOC and produces acetate and H_2, and the reactions of acetoclastic and hydrogenotrophic methanogenesis (Figure 1). The fermentation reaction can be described by the stoichiometric equation,

$$\mathrm{DOC} \rightarrow 2.7\mathrm{Acetate} + 1.2\mathrm{H_2} + \mathrm{CO_2} + 0.6\mathrm{H_2O} + 2.7\mathrm{H^+}. \quad (17)$$

At the end of their experiments, the amounts of SOM decomposed by microbes were relatively small, <1% of the SOM available at the beginning of the experiments (see Text S1). Therefore, we calculated the rates of SOM degradation by extracellular enzymes according to Equation 4. Furthermore, the acetoclastic pathway dominated methanogenesis, contributing to ~90% of total CH_4 production and leading to nearly equal production of CO_2 and CH_4. Therefore, we quantified the kinetics of anaerobic organic matter decomposition by using the rate of methane production.

We calibrated the model and achieved the possible ranges of the unknown model parameters by least-square fitting of the modeling results to the observations of the glucose-amended incubation experiments at 7°C, 15°C, and 25°C (Table 1). Specifically, the maximum apparent rate constant $k_{app,o}$ of enzymatic SOM degradation was estimated by minimizing the mean square error (MSE) between the simulated and observed temporal variations of DOC concentrations. The initial biomass concentration of fermenting microbes was obtained based on the variations in the concentrations of acetate and H_2. The initial biomass concentration of acetoclastic methanogens was estimated according to the concentrations of acetate, CH_4,

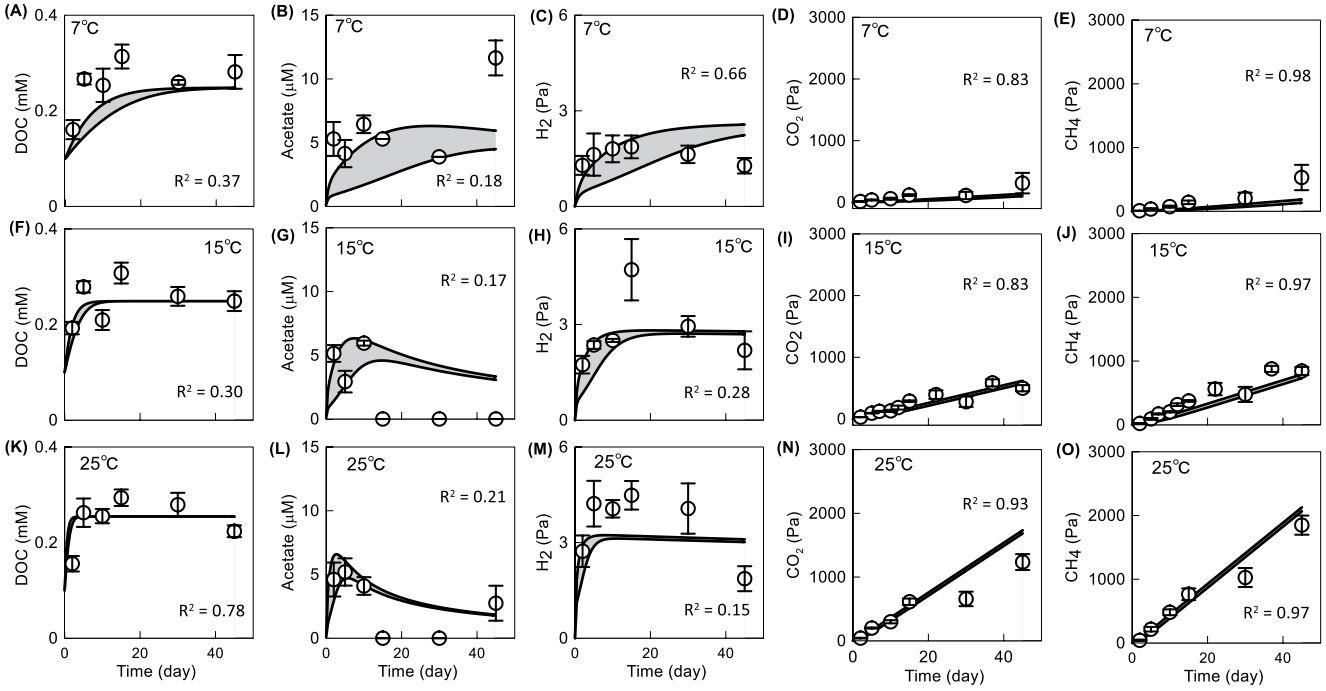

Figure 4. Model validation by applying the calibrated biogeochemical reaction model to the experiments of organic matter decomposition without glucose amendment at 7°C, 15°C, and 25°C. Data points are the concentrations of dissolved organic carbon (DOC), as represented by glucose empirically (A, F, K), acetate (B, G, L), H_2 (C, H, M), CO_2 (D, I, N), and CH_4 (E, J, O) reported by Ye et al. (2016); error bars show the 95% confidence intervals of the observations; solid lines and shaded areas are the simulation results by using the minimum and maximum initial biomass concentrations (see Table 1).

and CO_2. The initial biomass concentration of hydrogenotrophic methanogens was determined from the concentrations of H_2. The maximum biomass concentration of fermenting microbes was determined by fitting to the concentrations of DOC, CO_2, and CH_4. The minimum and optimal temperatures of the cardinal model were estimated on the basis of the concentrations of acetate, H_2, CH_4, and CO_2.

All simulations ran for 45 days, the same duration as the laboratory incubation experiments. Methane production rates were calculated from the total methane concentrations at day 45. Statistical analyses, including one-way ANOVA analysis and Spearman correlation, were conducted with python 3.7.

3. Results and Discussion

3.1. Biogeochemical Reaction Modeling

To simulate the temperature sensitivity of organic matter decomposition, we first constructed the biogeochemical reaction model by fitting the simulation results to the progress of organic matter decomposition in the glucose-amended experiments of Ye et al. (2016). The best-fit maximum apparent rate constant $k_{app,o}$ of enzymatic SOM degradation was $1.0 \pm 0.1 \times 10^{-2}$ mol · g^{-1} · s^{-1}, and the best-fit microbial parameters are listed in Table 1. These results are within the ranges of previous field and laboratory observations. In particular, the best-fit initial biomass concentrations are smaller than those determined in peatlands, for example, about 10 mg methanogens and 100 mg fermenting microbes per kg (dry weight) of peat (Horn et al., 2003; Jiang et al., 2010; Vester & Ingvorsen, 1998). The best-fit T_{min} is 0.0 ± 0.3°C, close to 2°C, the lowest temperature at which methanogens in Michigan peatlands remain metabolically active (Avery et al., 1999; Shannon & White, 1996). The best-fit T_{opt} is 27.0 ± 1.0°C, within the range of the optimal growth temperatures of mesophiles, from 20°C to 45°C (Robbins & Konhauser, 2021). As illustrated in Figure 3, the model simulation reproduces well the experimental results: DOC concentrations stabilize at ~0.22 mM; acetate and H_2 accumulate at the beginning of the experiments; CO_2 and CH_4 accumulate steadily over time.

We then validated the model by applying the biogeochemical reaction model, together with the best-fit model parameters (Table 1), to the glucose-free incubation experiments of Ye et al. (2016). As shown in Figure 4, without glucose amendment, DOC concentrations increase at the beginning of the experiments, and then stay constant at ~0.25 mM. Acetate and H_2 do not accumulate significantly, and their concentrations are more than one order of magnitude smaller than those in the glucose-amended experiments. CO_2 and CH_4 accumulate with time at rates slightly smaller than those in the glucose-amended experiments. Moreover, the simulation results suggest that acetoclastic methanogenesis accounts for approximately 90% of methane production, consistent with the laboratory assessment (Ye et al., 2012).

In both model construction and validation (Figures 3 and 4), the coefficient R^2 of determination for CH_4 and CO_2 are close to 1, but the R^2 of acetate and H_2 are relatively low (i.e., <0.7). The simulation results from the 95% confidence intervals of the initial biomass concentrations can cover the majority of the experimental results, except the temporal variations of acetate and H_2 concentrations. The mismatch between the simulated and observed concentrations is likely due to the technical challenge in analyzing low acetate and H_2 levels and the incomplete consideration of microbial reactions that consume and produce acetate and H_2, such as syntrophic metabolism and microbial reduction of sulfate and other external electron acceptors (Schink & Stams, 2013). In addition, among the different chemical species, acetate and H_2 respond most significantly to the variations in the initial biomass concentrations: by increasing the initial biomass concentrations from the minimum to the maximum values, acetate and H_2 concentrations increase up to 55% and 28%, respectively. Nevertheless, the model does capture the overall trends of acetate and H_2 concentrations, despite nearly two orders of magnitude concentration differences between the experiments of glucose amendment (Figure 3) and those without glucose addition (Figure 4). Combining these results, we conclude that the biogeochemical reaction model can be applied to simulate the temperature response of organic matter decomposition in the peatlands from the Upper Peninsula of Michigan.

The modeling results highlight the complexity of the organic matter decomposition even with our relatively simplified reaction network (Figure 1). First, among the three microbial functional groups, acetoclastic methanogens grow most significantly (Figures 5A–5C). Their biomass concentrations increase linearly with time, and the growth rates increase from 6.0×10^{-3} mg $\cdot$ kg^{-1} $\cdot$ d^{-1} at 7°C to 5.6×10^{-2} mg $\cdot$ kg^{-1} $\cdot$ d^{-1} at 25°C. At 7°C, the growth of fermenting microbes follows the same trend as those of acetoclastic methanogens, but at 15°C and 25°C, the growth is limited by the maximum biomass of 0.5 mg$\cdot$kg^{-1}. In comparison, the biomass concentrations of hydrogenotrophic methanogens do not respond significantly. The growth limitation of hydrogenotrophs is due to the limited H_2 production, whereas the limitation of fermenters is due to the holding capacity of the environment, the maximum biomass concentration supported by the environment. At the field sites, how physical and chemical conditions, such as nutrient concentrations and the availability and connectivity of space, lead to the limitation requires further investigation.

Second, the modeling results suggest that the organic matter decomposition can be separated into two phases, a dynamic phase followed by a stationary phase. In the dynamic phase, the enzymatic and microbial reaction rates and hence the rates of organic matter decomposition vary significantly. In the stationary phase, the rates remain nearly constant (Figures 5D–5G). The time required for reaching the stationary phase depends on temperature, and is 40, 15, and 10 days at 7°C, 15°C, and 25°C, respectively.

The variations in the reaction rates arise from changes in the environmental and biological factors. For example, variations in the enzymatic reaction rates result from the antagonistic effects of microbial growth and the accumulation of DOC. At the beginning of the experiments, the growth of fermenting microbes raises the rates (Figure 5A), but later into the experiments, the DOC accumulation (Figures 4A, 4F, and 4K) slows the process down.

Variations in fermentation rates (Figure 5D) match well with the variations in the biomass concentrations of fermenting microbes (Figure 5A), reflecting the controlling effect of biomass. Acetoclastic methanogenesis rates first increase and then remain constant. Although acetoclastic methanogen continues to grow in the stationary phase, the stimulatory effect of microbial growth is offset by the decrease in acetate concentrations (Figures 4B, 4G, and 4L) – another controlling factor of the methanogenesis rate. Our model also considers the limitation of the Gibbs free energy change. However, the free energies of the microbial

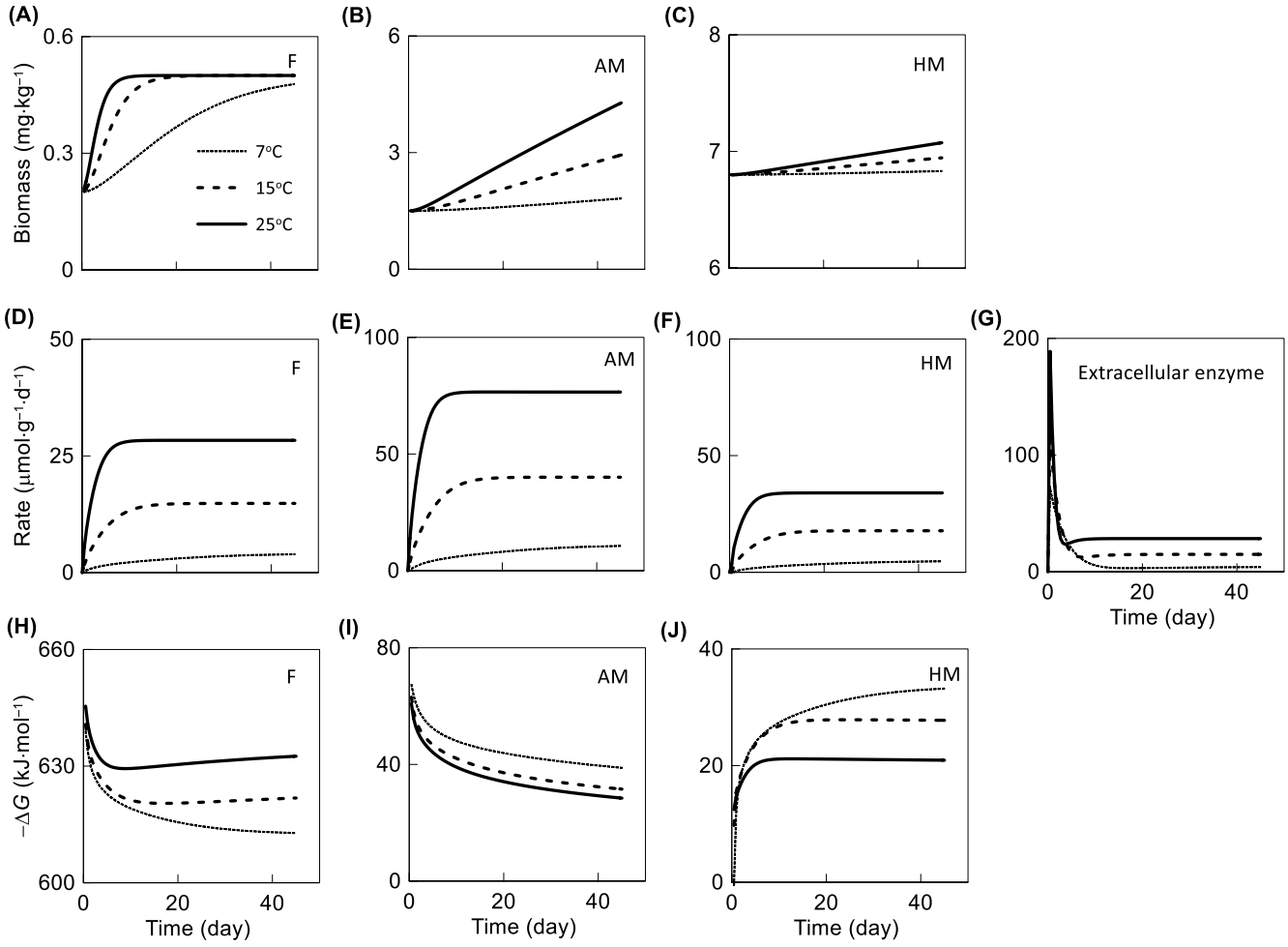

Figure 5. Variations with time in the biomass concentrations of fermenting microbes (F), acetoclastic (AM), and hydrogenotrophic methanogens (HM, panel A–C), reaction rates of fermentation, acetoclastic and hydrogenotrophic methanogenesis, and extracellular enzyme (panel D–G), and the Gibbs free energy change ΔG of fermentation reaction (Equation 17), and acetoclastic (Equation 6) and hydrogenotrophic methanogenesis reaction (Equation 7, panel H–J) at 7°C, 15°C, and 25°C.

reactions are much larger than the energies conserved by microbes (Figures 5H–5J), and hence have limited effect on microbial reactions rates.

We note that acetate accumulates throughout the incubation at 7°C (Figure 4B). At 15°C and 25°C, acetate accumulation is limited to the beginning of the experiments, the first 10 and 5 days, respectively, with empirical results showing even greater acetate depletion (Figures 4G and 4L). These results suggest that acetate production by fermentation is not fast enough to compensate for the consumption by acetoclastic methanogenesis at higher temperatures, consistent with the assumption that fermentation is the rate-determining step of anaerobic organic matter decomposition (Allison et al., 2010; Roy Chowdhury et al., 2015; Zheng et al., 2019).

3.2. Temperature Sensitivity

We applied the validated biogeochemical reaction model and simulated the organic matter degradation to CH_4 and CO_2 at different temperatures. Figures 6A and 6B show that, according to the simulation results, methane production responds to temperature variations by following an asymmetric unimodal curve, and can be described with the cardinal temperature model for mesophilic microbes (Equation 14). In particular, at temperatures <37°C, the production rate increases with increasing temperature and the increase is nearly linear between 5°C and 30°C ($R^2 = 0.98$). Between 37°C and 50°C, the rate decreases relatively fast

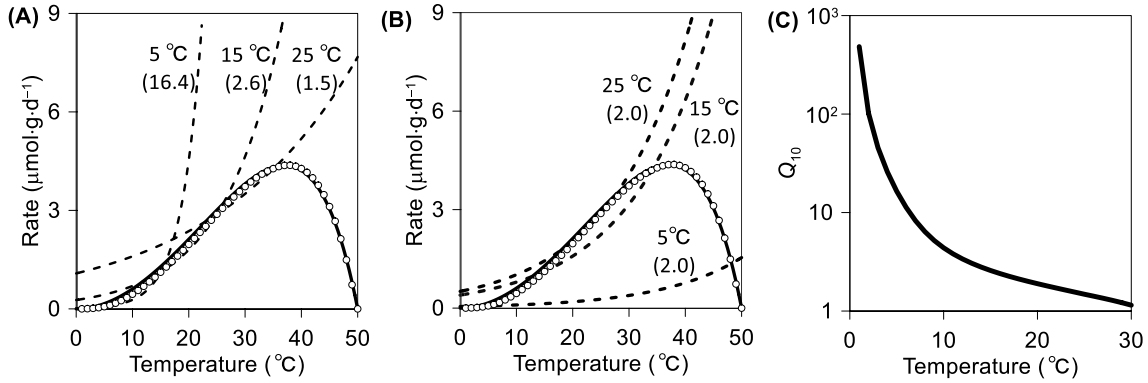

Figure 6. Variations with temperature in CH_4 production rate (A and B) and Q_{10} coefficient (C). In panels (A) and (B), data points represent the results of biogeochemical reaction modeling, and solid line is the product of the cardinal temperature model (Equation 14) and the maximum methane production rate obtained from the modeling, that is, 4.4 μmol · g^{-1} · d^{-1} at 37°C. Dashed lines in panel (A) are predictions according to the Q_{10} coefficients (labels in parentheses) and the basal rates obtained at 5, 15, and 25°C, and those in panel (B) are predictions by setting the Q_{10} coefficient at 2. In panel (C), line stands for the Q_{10} coefficients calculated according to the modeling results and Equation 1, and is plotted on a logarithmic scale.

with temperature. These results differ from the exponential responses assumed by the Q_{10} approach, but similar unimodal responses have been widely observed in previous laboratory incubation studies (Blake et al., 2015; Morrissey et al., 2014; Sha et al., 2011; Svensson, 1984). At temperatures <30°C, the nearly linear relationship has also been reported in peatlands (Avery et al., 2003; Bergman et al., 1998; Nykanen et al., 1998). Moreover, according to a meta-analysis of 376 laboratory incubation data sets, organic matter decomposition rates determined across different climate zones show a curvilinear relationship with incubation temperatures (Xu et al., 2016).

3.3. Q_{10} Approach

To apply the Q_{10} approach, we first calculated the Q_{10} coefficient from the modeling results (Figure 6C). Because methane production rate is 0 at 0°C, we calculate the Q_{10} coefficient between 1°C and 30°C. The coefficient is at its largest value, 484, at 1°C and decreases with increasing temperature. The initial decrease is fast; the Q_{10} coefficient drops to 3 at 13°C. Afterward, the decrease is modest, and the coefficient is near 1 at 30°C. At low temperatures, previous laboratory incubation studies have reported Q_{10} coefficients as large as 430 (Elberling & Brandt, 2003). According to our modeling results, these large Q_{10} values can be accounted for by relatively low rates of methane production at base temperatures (Equation 1). The decreasing Q_{10} coefficient with increasing temperature is consistent with the results of previous laboratory analyses. Hamdi et al. (2013) compiled the Q_{10} coefficients determined for aerobic CO_2 production (n = 317), and found that the Q_{10} values negatively correlate with temperatures, decreasing from >300 at about 0°C to 1.2 at 20°C.

We apply the Q_{10} coefficients to predict how rates of methane production vary with temperature. We first take 5°C, 15°C, and 25°C as examples, and calculate the rates by substituting into Equation 2 the basal rates r_o and the Q_{10} values determined at the three different temperatures (Figure 6A). The calculated rates at any particular temperature vary dramatically, depending on the base temperature used to determine the basal rate and the Q_{10} value. By comparing the predictions of the Q_{10} approach to the modeling results, we see that the Q_{10} approach tends to overestimate the rates of methane production.

We also calculate the rates by evaluating Equation 2 with the basal rates r_o at 5°C, 15°C, and 25°C and a constant Q_{10} coefficient of 2 (Figure 6B). The calculations also deviate significantly from the simulation results. The Q_{10} approach with the basal rate at 5°C tends to underestimate the simulated rates, while the calculations with the basal rate of 25°C tend to overestimate the rates. These results confirm that the constant Q_{10} approach brings in significant error in predicting the temperature response of methane production.

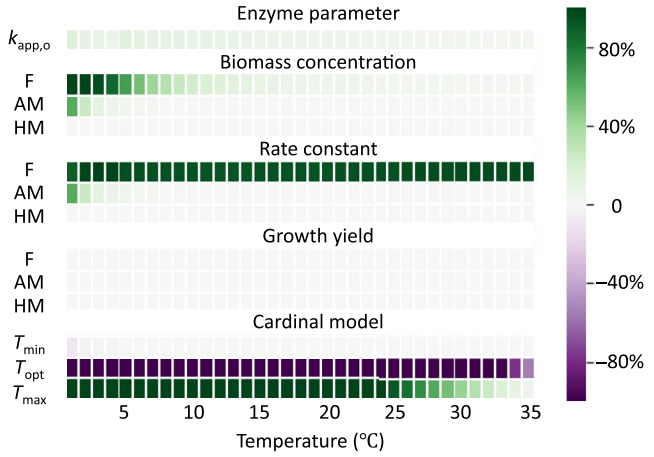

Figure 7. Variations with temperature in the scaled control coefficients of model parameters, including maximum rate constant $k_{app,o}$ of extracellular enzymes, biomass concentrations, rate constants, and growth yields of fermenting microbes (F), acetoclastic (AM), and hydrogenotrophic methanogens (HG), and the minimum (T_{min}), optimal (T_{opt}), and maximum temperatures (T_{max}) of the cardinal model for fermenting microbes. Control coefficients are calculated according to Equation 16.

3.4. Rate-Determining Step

Discrepancy between predictions of the Q_{10} and the modeling approaches arises mainly from the treatment of the temperature sensitivity of organic matter decomposition. The Q_{10} approach takes organic matter decomposition as a black box, and assumes that the decomposition rates vary with temperature according to the Arrhenius equation. This assumption does not hold according to the kinetics of enzymatic and microbial reactions. Both enzymatic and microbial reactions respond to temperature variations by following unimodal functions. As shown in Figures 2A and 2B, beyond the optimal temperatures for extracellular enzymes and microbes, the rates of enzymatic and microbial reactions no longer increase with increasing temperature.

Our modeling results support that the temperature response of anaerobic organic matter decomposition can be described according to the cardinal temperature model (Rossol et al., 1993). We account for this result with the limitation of anaerobic organic matter decomposition by the fermentation reactions that consume DOC (Allison et al., 2010; Roy Chowdhury et al., 2015; Zheng et al., 2019). We carried out a sensitivity analysis of the biogeochemical reaction model to evaluate the controlling effects of enzymatic and microbial reactions. Figure 7 shows the scaled control coefficients computed for the model parameters at different temperatures. Across the different temperatures, the control coefficient of the cell-specific maximum rate k of fermentation is 106 ± 8%, which indicates that the rate of organic matter decomposition varies proportionally with the rate constant of fermentation. The initial biomass concentration of fermenting microbes also has a relatively large control coefficient, ~80%, at <7°C, and the coefficient decreases gradually to 4% at 35°C. The control coefficient of fermentation growth yield ranges from 10–30% from 5°–15°C, and decreases to 3% at 35°C. Other model parameters do not control organic matter decomposition significantly. For example, the control coefficient of the apparent rate constant $k_{app,o}$ of the enzymatic reaction ranges from 14% at 5°C to 3% at 35°C. These results confirm that the anaerobic organic matter decomposition is limited by the fermentation reaction of DOC to acetate and H_2. In the biogeochemical reaction model, the fermentation reaction responds to temperature variations by following the cardinal temperature model, and so does the decomposition of SOM.

The rate limitation by the fermentation reaction suggests that the simulated temperature response of methane production depends on the parameters of the cardinal temperature model applied to the fermentation reaction. Figure 7 shows the scaled control coefficients of parameter T_{min}, T_{opt}, and T_{max} at temperatures ranging from 1°C to 35°C. While the control coefficient of T_{min} remains small, between −8% and 0, the control coefficient of T_{opt} stays <−50% across the different temperatures, and the coefficient of T_{max} is >80% at temperature <26°C. These results support the important and contrasting roles of T_{opt} and T_{max} in shaping the temperature response of methane production rates. According to the cardinal temperature model, increase in T_{opt} shifts the rate peak toward higher temperatures and, correspondingly, lowers the rates between T_{min} and T_{opt}. On the other hand, increase in T_{max} expands the unimodal relationship, thereby elevating the rates.

3.5. Meta-Data Analysis

A key outcome of our modeling exercise is that the cardinal temperature model provides a better description of the temperature response of methane production than the constant Q_{10} approach in the peatlands from the Upper Peninsula of Michigan, USA. To evaluate whether the cardinal temperature model is applicable to other field sites, we compiled the Q_{10} values of CO_2 (n = 109) and CH_4 (n = 190) production from anaerobic laboratory incubations (see https://zenodo.org/record/4480176, Wu et al., 2021b). Two patterns appear from the compilation. First, as shown in Figure 8A, methane production has a larger median Q_{10} value (2.9) than anaerobic CO_2 production (2.6). Second, according to the results of one-way ANOVA analysis with post-hoc Tukey's test (see Tables S1–S4), the Q_{10} values of CH_4 and CO_2 production differ significantly between different climate zones (p < 0.05, Figures 8B and 8C). In particular, the Q_{10} for CH_4 differs between

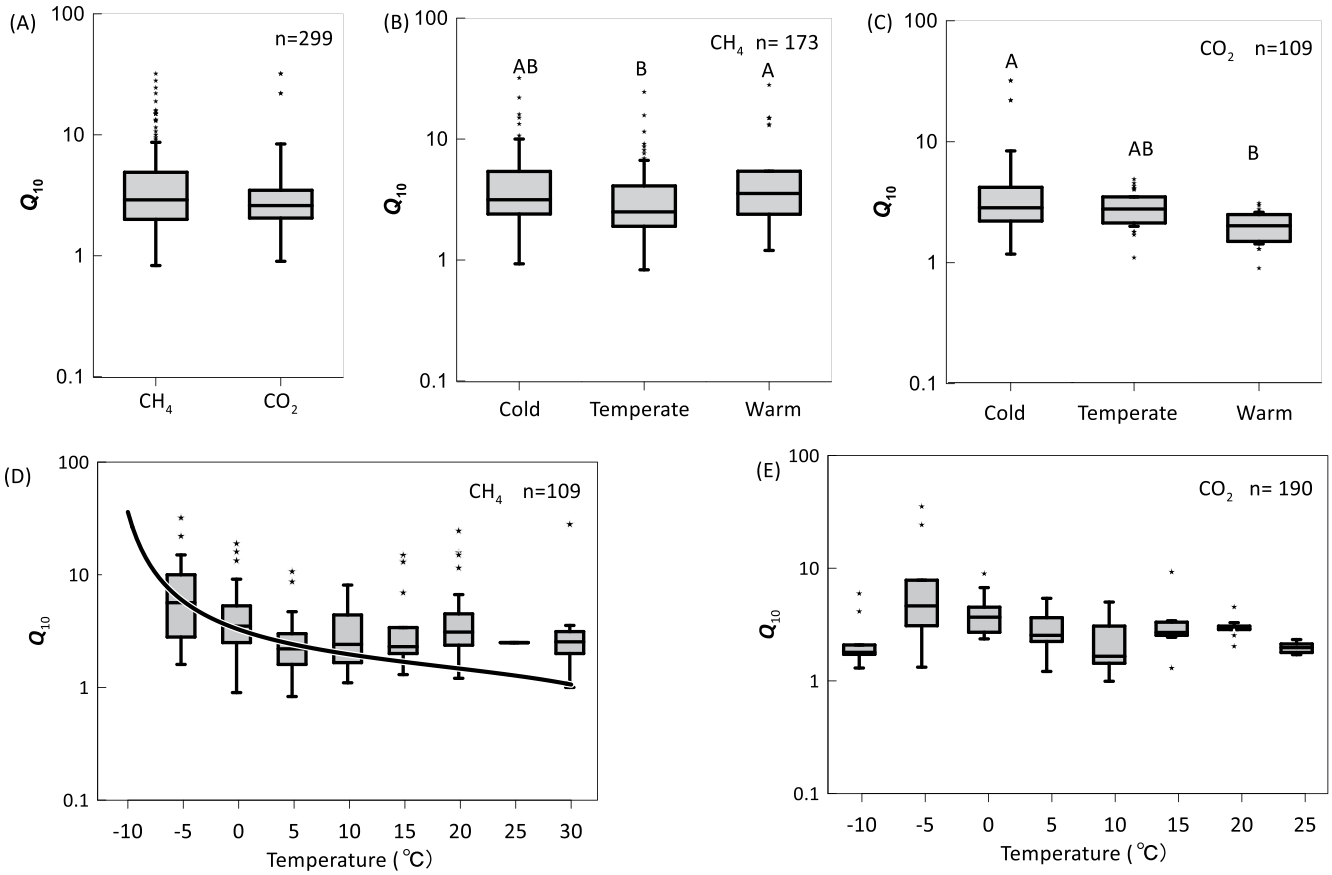

Figure 8. Q_{10} coefficients of anaerobic organic matter decomposition to CO_2 and CH_4 compiled from previous laboratory incubation studies. (A) Q_{10} coefficients of CH_4 production and CO_2 production. Q_{10} coefficients of CH_4 production (B) and CO_2 production (C) in different climate zones (only values with sampling locations are included). Q_{10} coefficients of CH_4 production (D) and CO_2 production (E) show significantly negative correlations with incubation temperatures (Spearman's coefficients of −0.51 and −0.25, respectively; $p < 0.05$). Box edges are the 25% and 75% percentiles of the data, horizontal center lines are median values, whisker bars show standard deviations, and star points are outliers. In panel (B) and (C), compact letter displays indicate the differences between groups ($p < 0.05$). In panel (D), solid line is the best-fit on the basis of the cardinal temperature model (Equation 18).

the temperature and warm zones, and the Q_{10} for CO_2 differs between cold and warm zones and marginally between cold and temperature zones ($p = 0.11$). In addition, Spearman correlation analyses show that Q_{10} coefficients of anaerobic CH_4 production and CO_2 production correlate negatively with incubation temperatures (Figures 8D and 8E). A notable example of this pattern is the 22 Q_{10} values obtained along a 3,800 km long north–south transect of forests in China, with low Q_{10} values in subtropical forests and high Q_{10} values in temperate forests (Wang et al., 2018).

The Q_{10} difference between anaerobic CO_2 and CH_4 production has been attributed to the availability of methanogenic substrates and alternative electron acceptors in the environment (Megonigal et al., 2003; Mu et al., 2018; Van Hulzen et al., 1999). Higher temperatures promote the degradation of SOM and increase the availability of H_2, acetate, and other methanogenic substrates, which in turn raises the temperature sensitivity of CH_4 production (Inglett et al., 2012). At the same time, higher temperatures also speed up microbial CO_2 production coupled to the reduction of ferric minerals, sulfate, and other external electron acceptors. Where these electron acceptors are limited, the temperature responses of CO_2 production are also limited. In addition, changes in temperatures shift the structure and function of microbial communities, which further contributes to the Q_{10} difference between CO_2 and CH_4 production (Auffret et al., 2016; Kolton et al., 2019). In our study, we did not include competing respiring microbial groups and, as a result, the simulated Q_{10} values of CO_2 and CH_4 productions are the same at given temperatures (results not shown).

The inverse relationship between Q_{10} and temperature has been accounted for by the differences in carbon quality or activation energy. In general, recalcitrant carbon tends to have larger activation energies

and hence large Q_{10} coefficients than labile carbon (Davidson & Janssens, 2006; Hilasvuori et al., 2013; Li et al., 2018). The availability of SOM also constrains the relationship. At high temperatures, SOM decomposition tends to be fast, which lowers the availability of SOM and therefore masks the intrinsic effect of temperature on decomposition rates, lowering the temperature sensitivity (Almulla et al., 2018; Gershenson et al., 2009; Inglett et al., 2012).

From the modeling perspective, the inverse relationship between Q_{10} and temperature supports the application of the cardinal temperature model beyond the peatlands from the Upper Peninsula of Michigan. To illustrate this point, we substitute Equation 14 to 1, and express Q_{10} coefficient in terms of the minimum, optimal, and maximum temperature of methane production,

$$Q_{10} = \frac{\left(T - T_{\max} + 10\right)\left(T - T_{\min} + 10\right)^2}{\left(T - T_{\max}\right)\left(T - T_{\min}\right)^2} \cdot \frac{\left(T - T_{\text{opt}}\right) - \left(T_{\text{opt}} - T_{\max}\right)\left(T_{\text{opt}} + T_{\min} - 2T\right)}{\left(T - T_{\text{opt}} + 10\right) - \left(T_{\text{opt}} - T_{\max}\right)\left(T_{\text{opt}} + T_{\min} - 2T - 20\right)}. \quad (18)$$

We then fit the equation to the median Q_{10} values from the compiled data set at different temperatures by fixing $T_{\max}$ at 50°C and by using nonlinear least squares fitting (Figure 8D). The best-fit $T_{\min}$ and T_{opt} are -12.0 ± 0.5 and 37.0 ± 12.4°C, respectively, and the MSE and R^2 are 1.36 and 0.80, respectively. The best-fit T_{opt} value falls within the range of the optimal temperatures of mesophiles, from 20° to 45°C (Hartel, 2005; Robbins & Konhauser, 2021). The best-fit $T_{\min}$ is lower than the $T_{\min}$ estimated above for the Michigan peatlands, and can be attributed to the inclusion of the Q_{10} values for arctic soils and other cold regions in the compiled data set.

The inverse relationship also supports a key assumption of our biogeochemical reaction model, microbial reactions respond to temperature variations by following the cardinal model. If we describe the temperature response of the fermentation reaction with a different model, such as the Arrhenius equation, we would still be able to reproduce the results of the laboratory incubation experiments (Figures S2 and S3). However, due to the rate-limiting effect of the fermentation reaction, the temperature response of methane production would follow the Arrhenius equation, resulting in a constant Q_{10} value at different temperatures (Figure S4).

4. Concluding Comments

We explored the temperature sensitivity of anaerobic organic matter decomposition using biogeochemical reaction modeling and compared the modeling results to those obtained from the Q_{10} approach. The biogeochemical reaction model presented here was constructed based on the catalytic mechanism of organic matter decomposition, a network of enzymatic and microbial reactions, and how the kinetics of individual reactions responds to temperature variations. The modeling results captured the influence of individual network reactions on anaerobic organic matter decomposition, and how the decomposition rates respond to the variations in temperature.

By applying both the biogeochemical reaction modeling and the Q_{10} approach to the peatlands in the Upper Peninsula of Michigan, USA, a number of differences arise:

1. Whereas Q_{10} approach treats organic matter decomposition as a black box, biogeochemical reaction modeling accounts for the underlying mechanism of organic matter decomposition, including the reactions of extracellular enzymes, fermentative microbes, and methanogens.
2. The Q_{10} approach builds on the Arrhenius equation that calculates rates of organic matter decomposition as an exponential function of temperature. In the biogeochemical reaction model, the temperature sensitivity of organic matter decomposition represents a systems property that arises from the interactions among enzymatic and microbial reactions in the entire biogeochemical reaction network.
3. In contrast to the exponential relationship predicted by the Q_{10} approach, the modeling results show that the temperature response of anaerobic organic matter decomposition follows the same pattern assumed for microbial reactions. In particular, between 5°C and 30°C, the decomposition rates vary almost linearly with temperature.

Our study helps make clear the extent to which the Q_{10} approach oversimplifies a complex biogeochemical process. As a result, the Q_{10} approach undermines the kinetic study of organic matter decomposition:

1. By neglecting the dynamics of organic matter decomposition. Most experimental studies determine Q_{10} coefficients from the accumulative CO_2 and CH_4 productions and the duration of the experiments are variable, from a couple of days to over months (Heslop et al., 2019; Lupascu et al., 2012). Because the rates of organic matter decomposition can vary with time, the Q_{10} coefficients obtained by using different incubation times can also be different.
2. By complicating the rate-temperature relationship of organic matter decomposition. As demonstrated by the modeling study here and by previous experimental efforts, the rates of organic matter decomposition do not necessarily vary with temperature exponentially. As a result, Q_{10} coefficients are not a constant, and a series of Q_{10} coefficients would be required to describe the rate-temperature relationship over the temperature ranges of interest.
3. By failing to provide an accurate description of the temperature sensitivity. Applying the Q_{10} approach requires the rate and the Q_{10} coefficient at a base temperature. However, at different temperatures, the rates and the Q_{10} coefficients are different, and there is no clear theoretical, or even empirical, rationale for choosing a particular base temperature.
4. By overestimating or underestimating the rates of organic matter decomposition, the Q_{10} applications introduce errors into the flux predictions of carbon cycling and their potential feedbacks to global climate.

Reliable prediction of reaction kinetics should account for catalytic mechanisms. The biogeochemical reaction model presented here is limited in that it is constructed for a specific field site, and hence does not include reactions that are potentially significant at other environments, such as respiration using external electron acceptors. It does not consider complicating physical and chemical factors (i.e., water content, organic matter accessibility, and so on) that influence the progress of organic matter decomposition (Gershenson et al., 2009, 2009; Wagai et al., 2013). Therefore, our results likely have simplified the temperature response of anaerobic organic matter decomposition. Nevertheless, from the dramatic differences between the modeling results and those given by the Q_{10} approach, we can conclude that the Q_{10} coefficient may not be effective as a parameter for quantifying the temperature sensitivity of organic matter decomposition. We also suggest that biogeochemical reaction modeling, combined with laboratory incubation experiments, can be applied to integrate more realistic description of reaction mechanisms into the kinetic study of organic matter decomposition and to uncover the relationship between organic matter decomposition rates and the temperature of the environment.

Conflict of Interest

The authors declare no conflicts of interest relevant to this study.

Data Availability Statement

The amended thermodynamic database, the input PHREEQC scripts for this research, and the compiled data set of temperature sensitivity of anaerobic CO_2 and CH_4 production are available from Zenodo at https://zenodo.org/record/4480176 (DOI: 10.5281/zenodo.4480066, and 10.5281/zenodo.4480221).

Acknowledgments
This research was funded by the National Science Foundation under award EAR-1636815 and 1753436 and by National Aeronautics and Space Administration under grant NNX16AJ59G.

References

Aderibigbe, E. Y., & Odunfa, S. A. (1990). Growth and extracellular enzyme production by strains of Bacillus species isolated from fermenting African locust bean, iru. *Journal of Applied Bacteriology*, *69*(5), 662–671. https://doi.org/10.1111/j.1365-2672.1990.tb01560.x

Allison, S. D., Wallenstein, M. D., & Bradford, M. A. (2010). Soil-carbon response to warming dependent on microbial physiology. *Nature Geoscience*, *3*(5), 336–340. https://doi.org/10.1038/ngeo846

Almulla, A., Jones, D., & Roberts, P. (2018). Substrate influences temperature sensitivity of dissolved organic carbon (DOC) and nitrogen (DON) mineralization in arid agricultural soils. *Soil Systems*, *2*(2), 28. https://doi.org/10.3390/soilsystems2020028

Alster, C. J., Baas, P., Wallenstein, M. D., Johnson, N. G., & von Fischer, J. C. (2016). Temperature sensitivity as a microbial trait using parameters from macromolecular rate theory. *Frontiers in Microbiology*, *7*, 1–10. https://doi.org/10.3389/fmicb.2016.01821

Auffret, M. D., Karhu, K., Khachane, A., Dungait, J. A. J., Fraser, F., Hopkins, D. W., et al. (2016). The role of microbial community composition in controlling soil respiration responses to temperature. *PloS One*, *11*(10), 1–19. https://doi.org/10.1371/journal.pone.0165448

Avery, G. B., Shannon, R. D., White, J. R., Christopher, S., Alperin, M. J., Jr, G. B. A., & Jeffrey, R. (2003). Production via acetate fermentation and CO_2 reduction controls on methane production in a tidal freshwater estuary and a peatland : Methane production via acetate fermentation and CO, reduction. *Production*, *62*(1), 19–37. https://doi.org/10.1023/a:1021128400602

Avery, G. B., Shannon, R. D., White, J. R., Martens, C., & Alperin, M. J. (1999). Effect of seasonal changes in the pathways of methanogenesis on the $\delta^{13}C$ values of pore water methane in a Michigan peatland. *Global Biogeochemical Cycles*, *13*(2), 475–484. https://doi.org/10.1029/1999GB900007

Bergman, I., Svensson, B. H., & Nilsson, M. (1998). Regulation of methane production in a Swedish acid mire by pH, temperature and substrate. *Soil Biology and Biochemistry*, *30*(6), 729–741. https://doi.org/10.1016/S0038-0717(97)00181-8

Blake, L. I., Tveit, A., Øvreås, L., Head, I. M., & Gray, N. D. (2015). Response of methanogens in arctic sediments to temperature and methanogenic substrate availability. *PloS One*, *10*(6), 1–18. https://doi.org/10.1371/journal.pone.0129733

Burns, R. G., DeForest, J. L., Marxsen, J., Sinsabaugh, R. L., Stromberger, M. E., Wallenstein, M. D., et al. (2013). Soil enzymes in a changing environment: Current knowledge and future directions. *Soil biology and biochemistry*. Pergamon. https://doi.org/10.1016/j.soilbio.2012.11.009

Charlton, S. R., & Parkhurst, D. L. (2011). Modules based on the geochemical model PHREEQC for use in scripting and programming languages. *Computers & Geosciences*, *37*(10), 1653–1663. https://doi.org/10.1016/j.cageo.2011.02.005

Ciais, P., Sabine, C., Bala, G., Bopp, L., Brovkin, V., Canadell, J., et al. (2013). The physical science basis. Contribution of working group I to the fifth assessment report of the intergovernmental panel on climate change. *Change, IPCC climate* (pp. 465–570). https://doi.org/10.1017/CBO9781107415324.015

Davidson, E. A., & Janssens, I. A. (2006). Temperature sensitivity of soil carbon decomposition and feedbacks to climate change. *Nature*, *440*(7081), 165–173. https://doi.org/10.1177/0146621684008003091O.1038/nature04514

DeLong, J. P., Gibert, J. P., Luhring, T. M., Bachman, G., Reed, B., Neyer, A., & Montooth, K. L. (2017). The combined effects of reactant kinetics and enzyme stability explain the temperature dependence of metabolic rates. *Ecology and Evolution*, *7*(11), 3940–3950. https://doi.org/10.1002/ece3.2955

Elberling, B., & Brandt, K. K. (2003). Uncoupling of microbial CO_2 production and release in frozen soil and its implications for field studies of arctic C cycling. *Soil Biology and Biochemistry*, *35*(2), 263–272. https://doi.org/10.1016/S0038-0717(02)00258-4

Eyring, H. (1935). The activated complex in chemical reactions. *The Journal of Chemical Physics*, *3*, 107–115. https://doi.org/10.1063/1.1749604

Fell, D. A. (1992). Metabolic control analysis: A survey of its theoretical and experimental development. *Biochemical Journal*, *286*. https://doi.org/10.1042/bj2860313

Feller, G. (2010). Protein stability and enzyme activity at extreme biological temperatures. *Journal of Physics: Condensed Matter*, *22*(32). https://doi.org/10.1088/0953-8984/22/32/323101

Finke, N., & Jørgensen, B. B. (2008). Response of fermentation and sulfate reduction to experimental temperature changes in temperate and Arctic marine sediments. *The ISME Journal*, *2*(8), 815–829. https://doi.org/10.1038/ismej.2008.20

Fissore, C., Giardina, C. P., Kolka, R. K., Trettin, C. C., King, G. M., Jurgensen, M. F., et al. (2008). Temperature and vegetation effects on soil organic carbon quality along a forested mean annual temperature gradient in North America. *Global Change Biology*, *14*(1), 193–205. https://doi.org/10.1111/j.1365-2486.2007.01478.x

Foereid, B., Ward, D. S., Mahowald, N., Paterson, E., & Lehmann, J. (2014). The sensitivity of carbon turnover in the community land model to modified assumptions about soil processes. *Earth System Dynamics*, *5*(1), 211–221. https://doi.org/10.5194/esd-5-211-2014

Gershenson, A., Bader, N. E., & Cheng, W. (2009). Effects of substrate availability on the temperature sensitivity of soil organic matter decomposition. *Global Change Biology*, *15*(1), 176–183. https://doi.org/10.1111/j.1365-2486.2008.01827.x

Gill, A. L., Giasson, M. A., Yu, R., & Finzi, A. C. (2017). Deep peat warming increases surface methane and carbon dioxide emissions in a black spruce-dominated ombrotrophic bog. *Global Change Biology*, *23*(12), 5398–5411. https://doi.org/10.1111/gcb.13806

Gueguen, Y., Chemardin, P., Arnaud, A., & Galzy, P. (1995). Comparative study of extracellular and intracellular β-glucosidases of a new strain of Zygosaccharomyces bailii isolated from fermenting agave juice. *Journal of Applied Bacteriology*, *78*(3), 270–280. https://doi.org/10.1111/j.1365-2672.1995.tb05026.x

Hagerty, S. B., Van Groenigen, K. J., Allison, S. D., Hungate, B. A., Schwartz, E., Koch, G. W., et al. (2014). Accelerated microbial turnover but constant growth efficiency with warming in soil. *Nature Climate Change*, *4*(10), 903–906. https://doi.org/10.1038/nclimate2361

Hamdi, S., Moyano, F., Sall, S., Bernoux, M., & Chevallier, T. (2013). Synthesis analysis of the temperature sensitivity of soil respiration from laboratory studies in relation to incubation methods and soil conditions. *Soil Biology and Biochemistry*, *58*, 115–126. https://doi.org/10.1016/j.soilbio.2012.11.012

Hartel, P. G. (2005). Microbial processes: Environmental factors. In D. Hillel (Ed.) *Encyclopedia of soils in the environment* (pp. 448–455). Oxford: Elsevier. https://doi.org/10.1016/B0-12-348530-4/00155-7

Heitzer, A., Kohler, H. P. E., Reichert, P., & Hamer, G. (1991). Utility of phenomenological models for describing temperature dependence of bacterial growth. *Applied and Environmental Microbiology*, *57*(9), 2656–2665. https://doi.org/10.1128/aem.57.9.2656-2665.1991

Heslop, J. K., Walter Anthony, K. M., Grosse, G., Liebner, S., & Winkel, M. (2019). Century-scale time since permafrost thaw affects temperature sensitivity of net methane production in thermokarst-lake and talik sediments. *The Science of the Total Environment*, *691*, 124–134. https://doi.org/10.1016/j.scitotenv.2019.06.402

Hilasvuori, E., Akujärvi, A., Fritze, H., Karhu, K., Laiho, R., Mäkiranta, P., et al. (2013). Temperature sensitivity of decomposition in a peat profile. *Soil Biology and Biochemistry*, *67*, 47–54. https://doi.org/10.1016/j.soilbio.2013.08.009

Hoehler, T. M., & Jørgensen, B. B. (2013). Microbial life under extreme energy limitation. *Nature reviews microbiology*. Nature Publishing Group. https://doi.org/10.1038/nrmicro2939

Hopkins, F. M., Filley, T. R., Gleixner, G., Lange, M., Top, S. M., & Trumbore, S. E. (2014). Increased belowground carbon inputs and warming promote loss of soil organic carbon through complementary microbial responses. *Soil Biology and Biochemistry*, *76*, 57–69. https://doi.org/10.1016/j.soilbio.2014.04.028

Hopple, A. M., Wilson, R. M., Kolton, M., Zalman, C. A., Chanton, J. P., Kostka, J., et al. (2020). Massive peatland carbon banks vulnerable to rising temperatures. *Nature Communications*, *11*(1), 4–10. https://doi.org/10.1038/s41467-020-16311-8

Horn, M. A., Matthies, C., Küsel, K., Schramm, A., & Drake, H. L. (2003). Hydrogenotrophic methanogenesis by moderately acid-tolerant methanogens of a methane-emitting acidic peat. *Applied and Environmental Microbiology*, *69*(1), 74–83. https://doi.org/10.1128/AEM.69.1.74-83.2003

Hungate, R. E. (1967). Hydrogen as an intermediate in the rumen fermentation. *Archiv für Mikrobiologie*, *59*(1–3), 158–164. https://doi.org/10.1007/bf00406327

Inglett, K. S., Inglett, P. W., Reddy, K. R., & Osborne, T. Z. (2012). Temperature sensitivity of greenhouse gas production in wetland soils of different vegetation. *Biogeochemistry*, *108*(1–3), 77–90. https://doi.org/10.1007/s10533-011-9573-3

Jackson, R. B., Saunois, M., Bousquet, P., Canadell, J. G., Poulter, B., Stavert, A. R., et al. (2020). Increasing anthropogenic methane emissions arise equally from agricultural and fossil fuel sources. *Environmental Research Letters*, *15*(7). https://doi.org/10.1088/1748-9326/ab9ed2

Jiang, N., Wang, Y., & Dong, X. (2010). Methanol as the primary methanogenic and acetogenic precursor in the cold Zoige wetland at Tibetan Plateau. *Microbial Ecology*, *60*(1), 206–213. https://doi.org/10.1007/s00248-009-9602-0

Jin, Q., & Bethke, C. M. (2003). A new rate law describing microbial respiration. *Applied and Environmental Microbiology*, *69*(4), 2340–2348. https://doi.org/10.1128/AEM.69.4.2340-2348.2003

Jin, Q., & Bethke, C. M. (2005). Predicting the rate of microbial respiration in geochemical environments. *Geochimica et Cosmochimica Acta*, *69*(5), 1133–1143. https://doi.org/10.1016/j.gca.2004.08.010

Jin, Q., & Kirk, M. F. (2018). pH as a primary control in environmental microbiology: 2. Kinetic perspective. *Frontiers in Environmental Science*, *6*, 1–16. https://doi.org/10.3389/fenvs.2018.00101

Jin, Q., & Roden, E. E. (2011). Microbial physiology-based model of ethanol metabolism in subsurface sediments. *Journal of Contaminant Hydrology*, *125*(1–4), 1–12. https://doi.org/10.1016/j.jconhyd.2011.04.002

Kim, Y., Ingram, L. O., & Shanmugam, K. T. (2007). Construction of an Escherichia coli K-12 mutant for homoethanologenic fermentation of glucose or xylose without foreign genes. *Applied and Environmental Microbiology*, *73*(6), 1766–1771. https://doi.org/10.1128/AEM.02456-06

Kolton, M., Marks, A., Wilson, R. M., Chanton, J. P., & Kostka, J. E. (2019). Impact of warming on greenhouse gas production and microbial diversity in anoxic peat from a Sphagnum-dominated bog (Grand Rapids, Minnesota, United States). *Frontiers in Microbiology*, *10*, 1–13. https://doi.org/10.3389/fmicb.2019.00870

Lee, H. S., Salerno, M. B., & Rittmann, B. E. (2008). Thermodynamic evaluation on H2 production in glucose fermentation. *Environmental Science and Technology*, *42*(7), 2401–2407. https://doi.org/10.1021/es702610v

Li, J., Yan, D., Pendall, E., Pei, J., Noh, N. J., He, J. S., et al. (2018). Depth dependence of soil carbon temperature sensitivity across Tibetan permafrost regions. *Soil Biology and Biochemistry*, *126*(August), 82–90. https://doi.org/10.1016/j.soilbio.2018.08.015

Lupascu, M., Wadham, J., Hornibrook, E., & Pancost, R. (2012). Temperature sensitivity of methane production in the permafrost active layer at Stordalen, Sweden: A comparison with non-permafrost Northern Wetlands. *Arctic Antarctic and Alpine Research*, *44*(4), 469–482. https://doi.org/10.1657/1938-4246-44.4.469

Megonigal, J. P., Hines, M. E., & Visscher, P. T. (2003). In H. D. Holland & K. K. B. T. Turekian (Eds.) *Anaerobic metabolism: Linkages to trace gases and aerobic processes* (pp. 317–424). Oxford: Pergamon. https://doi.org/10.1016/B0-08-043751-6/08132-9

Morrissey, E. M., Berrier, D. J., Neubauer, S. C., & Franklin, R. B. (2014). Using microbial communities and extracellular enzymes to link soil organic matter characteristics to greenhouse gas production in a tidal freshwater wetland. *Biogeochemistry*, *117*(2–3), 473–490. https://doi.org/10.1007/s10533-013-9894-5

Mu, C., Li, L., Wu, X., Zhang, F., Jia, L., Zhao, Q., & Zhang, T. (2018). Greenhouse gas released from the deep permafrost in the northern Qinghai-Tibetan Plateau. *Scientific Reports*, *8*(1), 1–9. https://doi.org/10.1038/s41598-018-22530-3

Nykanen, H., Alm, J., Silvola, J., Tolonen, K., & Martikainen, P. J. (1998). Methane fluxes on boreal peatlands of different fertility and the effect of long-term experimental lowering of the water table on flux rates. *Global Biogeochemical Cycles*, *12*(1), 53–69. https://doi.org/10.1029/97GB02732

Parashar, C. D., Gupta, K. P., Rai, J., Sharma, C. R., & Singh, N. (1993). Effect of soil temperature on methane emission from paddy fields. *Chemosphere*, *26*(1–3), 247–250. https://doi.org/10.1016/0045-6535(93)90425-5

Perkins, D. M., Yvon-Durocher, G., Demars, B. O. L., Reiss, J., Pichler, D. E., Friberg, N., et al. (2012). Consistent temperature dependence of respiration across ecosystems contrasting in thermal history. *Global Change Biology*, *18*(4), 1300–1311. https://doi.org/10.1111/j.1365-2486.2011.02597.x

Price, P. B., & Sowers, T. (2004). Temperature dependence of metabolic rates for microbial growth, maintenance, and survival. *Proceedings of the National Academy of Sciences*, *101*(13), 4631–4636. https://doi.org/10.1073/pnas.0400522101

Raich, J. W., Russell, E. A., Kitayama, K., Parton, J. W., & Vitousek, M. P. (2006). Temperature influences carbon accumulation in moist tropical forests. *Ecology*, *87*(1), 76–87. https://doi.org/10.1890/05-0023

Ratkowsky, D. A., Lowry, R. K., McMeekin, T. A., Stokes, A. N., & Chandler, R. E. (1983). Model for bacterial culture growth rate throughout the entire biokinetic temperature range. *Journal of Bacteriology*, *154*(3), 1222–1226. https://doi.org/10.1128/jb.154.3.1222-1226.1983

Robbins, L. J., & Konhauser, K. O. (2021). Geobiology and Geomicrobiology. *Encyclopedia of geology* (pp. 554–568). Elsevier. https://doi.org/10.1016/b978-0-12-409548-9.12532-1

Romero-Olivares, A. L., Allison, S. D., & Treseder, K. K. (2017). Soil microbes and their response to experimental warming over time: A meta-analysis of field studies. *Soil Biology and Biochemistry*, *107*, 32–40. https://doi.org/10.1016/j.soilbio.2016.12.026

Rossol, L., Lobry, J. R., & Flandrois, J. P. (1993). An unexpected correlation between cardinal temperatures of microbial growth highlighted by a new model. *Journal of Theoretical Biology*, *162*, 447–463. https://doi.org/10.1006/jtbi.1993.1099

Roy Chowdhury, T., Herndon, E. M., Phelps, T. J., Elias, D. A., Gu, B., Liang, L., et al. (2015). Stoichiometry and temperature sensitivity of methanogenesis and CO_2 production from saturated polygonal tundra in Barrow, Alaska. *Global Change Biology*, *21*(2), 722–737. https://doi.org/10.1111/gcb.12762

Schink, B. (1997). Energetics of syntrophic cooperation in methanogenic degradation. *Microbiology and Molecular Biology Reviews: Microbiology and Molecular Biology Reviews*, *61*(2), 262–280. https://doi.org/10.1128/.61.2.262-280.1997

Schink, B., & Stams, A. (2013). In E. Rosenberg (Ed.), *Syntrophism among prokaryotes in the Prokaryotes* (pp. 471–493). https://doi.org/10.1007/978-3-642-30123-0_59

Schipper, L. A., Hobbs, J. K., Rutledge, S., & Arcus, V. L. (2014). Thermodynamic theory explains the temperature optima of soil microbial processes and high Q_{10} values at low temperatures. *Global Change Biology*, *20*(11), 3578–3586. https://doi.org/10.1111/gcb.12596

Sha, C., Mitsch, W. J., Mander, Ü., Lu, J., Batson, J., Zhang, L., & He, W. (2011). Methane emissions from freshwater riverine wetlands. *Ecological Engineering*, *37*(1), 16–24. https://doi.org/10.1016/j.ecoleng.2010.07.022

Shannon, R. D., & White, J. R. (1996). The effects of spatial and temporal variations in acetate and sulfate on methane cycling in two Michigan peatlands. *Limnology & Oceanography*, *41*(3), 435–443. https://doi.org/10.4319/lo.1996.41.3.0435

Shiloach, J., Kaufman, J., Guillard, A. S., & Fass, R. (1996). Effect of glucose supply strategy on acetate accumulation, growth, and recombinant protein production by Escherichia coli BL21 (λDE3) and Escherichia coli JM109. *Biotechnology and Bioengineering*, *49*(4), 421–428. https://doi.org/10.1002/(SICI)1097-0290(19960220)49:4<421::AID-BIT9>3.0.CO;2-R

Singh, V., & Das, D. (2019). Chapter 3: Potential of hydrogen production from biomass. In P. E. V. de Miranda (Ed.) *Science and engineering of hydrogen-based energy technologies : Hydrogen production and practical applications in energy generation* (pp. 123–164). Academic Press. https://doi.org/10.1016/B978-0-12-814251-6.00003-4

Stams, A. J. M., Elferink, S. J. W. H. O., & Westermann, P. (2003). Metabolic interactions between methanogenic consortia and anaerobic respiring bacteria. In B. K. Ahring, I. Angelidaki, E. C. de Macario, H. N. Gavala, J. Hofman-Bang, A. J. L. Macario, et al. (Eds.), *Biomethanation I* (pp. 31–56). Berlin, Heidelberg: Springer Berlin Heidelberg. https://doi.org/10.1007/3-540-45839-5_2

Stone, M. M., Weiss, M. S., Goodale, C. L., Adams, M. B., Fernandez, I. J., German, D. P., & Allison, S. D. (2012). Temperature sensitivity of soil enzyme kinetics under N-fertilization in two temperate forests. *Global Change Biology*, *18*(3), 1173–1184. https://doi.org/10.1111/j.1365-2486.2011.02545.x

Svensson, B. H. (1984). Different temperature optima for methane formation when enrichments from acid peat are supplemented with acetate or hydrogen. *Applied and Environmental Microbiology*, *48*(2), 389–394. https://doi.org/10.1128/aem.48.2.389-394.1984

Tang, G., Zheng, J., Xu, X., Yang, Z., Graham, D. E., Gu, B., et al. (2016). Biogeochemical modeling of CO_2 and CH_4 production in anoxic Arctic soil microcosms. *Biogeosciences*, *13*(17), 5021–5041. https://doi.org/10.5194/bg-13-5021-2016

Thauer, R. K., Kaster, A. K., Seedorf, H., Buckel, W., & Hedderich, R. (2008). Methanogenic archaea: Ecologically relevant differences in energy conservation. *Nature Reviews Microbiology*, *6*(8), 579–591. https://doi.org/10.1038/nrmicro1931

Todd-brown, K. E. O., Zheng, B., & Crowther, T. W. (2018). Field-warmed soil carbon changes imply high 21st-century modeling uncertainty. *Biogeosciences*, *15*, 3659–3671. https://doi.org/10.3929/ethz-a-01078258110.5194/bg-15-3659-2018

Van Hulzen, J. B., Segers, R., Van Bodegom, P. M., & Leffelaar, P. A. (1999). Temperature effects on soil methane production: An explanation for observed variability. *Soil Biology and Biochemistry*, *31*(14), 1919–1929. https://doi.org/10.1016/S0038-0717(99)00109-1

van't Hoff, J. H. (1898). *Lectures in theoretical and physical chemistry : Part I : Chemical dynamics LK* (p. 256). London: Edward Arnold. https://UOLibraries.on.worldcat.org/oclc/220605730

Vester, F., & Ingvorsen, K. (1998). Improved Most-Probable-Number Method To Detect Sulfate-Reducing Bacteria with Natural Media and a Radiotracer. *Applied and Environmental Microbiology*, *64*. https://doi.org/10.1128/aem.64.5.1700-1707.1998

von Lützow, M., & Kögel-Knabner, I. (2009). Temperature sensitivity of soil organic matter decomposition-what do we know? *Biology and Fertility of Soils*, *46*, 1–15. https://doi.org/10.1007/s00374-009-0413-8

Wagai, R., Kishimoto-Mo, A. W., Yonemura, S., Shirato, Y., Hiradate, S., & Yagasaki, Y. (2013). Linking temperature sensitivity of soil organic matter decomposition to its molecular structure, accessibility, and microbial physiology. *Global Change Biology*, *19*(4), 1114–1125. https://doi.org/10.1111/gcb.12112

Wang, Q., Liu, S., & Tian, P. (2018). Carbon quality and soil microbial property control the latitudinal pattern in temperature sensitivity of soil microbial respiration across Chinese forest ecosystems. *Global Change Biology*, *24*(7), 2841–2849. https://doi.org/10.1111/gcb.14105

Wu, Q., Ye, R., Bridgham, S., & Jin, Q. (2021a). *Phreeqc script*. https://doi.org/10.5281/zenodo.4480176

Wu, Q., Ye, R., Bridgham, S., & Jin, Q. (2021b). *Q10 dataset*. https://doi.org/10.5281/zenodo.4480066

Xu, X., Shi, Z., Li, D., Rey, A., Ruan, H., Craine, J. M., et al. (2016). Soil properties control decomposition of soil organic carbon: Results from data-assimilation analysis. *Geoderma*, *262*, 235–242. https://doi.org/10.1016/j.geoderma.2015.08.038

Ye, R., Jin, Q., Bohannan, B., Keller, J. K., McAllister, S. A., & Bridgham, S. D. (2012). PH controls over anaerobic carbon mineralization, the efficiency of methane production, and methanogenic pathways in peatlands across an ombrotrophic-minerotrophic gradient. *Soil Biology and Biochemistry*, *54*, 36–47. https://doi.org/10.1016/j.soilbio.2012.05.015

Ye, R., Keller, J. K., Jin, Q., Bohannan, B. J. M., & Bridgham, S. D. (2016). Peatland types influence the inhibitory effects of a humic substance analog on methane production. *Geoderma*, *265*, 131–140. https://doi.org/10.1016/j.geoderma.2015.11.026

Zheng, J., Thornton, P. E., Painter, S. L., Gu, B., Wullschleger, S. D., & Graham, D. E. (2019). Modeling anaerobic soil organic carbon decomposition in Arctic polygon tundra: Insights into soil geochemical influences on carbon mineralization. *Biogeosciences*, *16*(3), 663–680. https://doi.org/10.5194/bg-16-663-2019

References From the Supporting Information

Bridgham, S. D., Updegraff, K., & Pastor, J. (1998). Carbon, nitrogen, and phosphorus mineralization in northern wetlands. *Ecology*, *79*(5), 1545–1561. https://doi.org/10.1890/0012-9658(1998)079[1545:CNAPMI]2.0.CO;2

Johnson, J. W., Oelkers, E. H., & Helgeson, H. C. (1992). SUPCRT92: A software package for calculating the standard molal thermodynamic properties of minerals, gases, aqueous species, and reactions from 1 to 5000 bar and 0 to 1000°C. *Computers & Geosciences*, *18*. https://doi.org/10.1016/0098-3004(92)90029-Q